

Anomalies in bulk supercooled water at negative pressure

Gaël Pallares¹, Mouna El Mekki Azouzi¹, Miguel Angel Gonzalez², Juan Luis Aragonés², Jose Luis F. Abascal², Chantal Valeriani² and Frédéric Caupin¹

¹*Institut Lumière Matière, UMR5306 Université Lyon 1-CNRS, Université de Lyon, Institut universitaire de France 69622 Villeurbanne Cedex, France and*

²*Departamento de Química Física I, Facultad de Ciencias Químicas, Universidad Complutense, 28040 Madrid, Spain*

(Dated: 27 November 2013)

Water is the most familiar liquid, and arguably the most complex. Anomalies of supercooled water have been measured during decades, and competing interpretations proposed. Yet, a decisive experiment remains elusive, because of unavoidable crystallization into ice. We investigate the state of water that is both supercooled and under mechanical tension, or negative pressure. Liquids under negative pressure can be found in plants or fluid inclusions in minerals. Using such water inclusions in quartz, we report the first measurements on doubly metastable water down to -15°C and around -100 MPa . We observe sound velocity anomalies that can be reproduced quantitatively with molecular dynamics simulations. These results rule out one proposed scenario for water anomalies, and put further constraints on the remaining ones.

Water differs in many ways from standard liquids: ice floats on water, and, upon cooling below 4°C , the liquid density decreases. In the supercooled liquid, many quantities, for example heat capacity and isothermal compressibility, show a large increase. Extrapolation of experimental data suggested a power-law divergence of these quantities at -45°C ¹. Thirty years ago, the stability-limit conjecture proposed that an instability of the liquid would cause the divergence² (Fig. 1a). This is supported by equations of state (EoSs), such as the IAPWS EoS³, fitted on the stable liquid and extrapolated to the metastable regions. Ten years later, the second critical point interpretation, based on simulations⁴, proposed that, instead of diverging, the anomalous quantities would reach a peak, near a Widom line^{5,6} that emanates from a critical point terminating a first order transition between two distinct liquid phases at low temperature (Fig. 1b). The two scenarios differ in the shape of the line of density maxima (LDM) of water (see Fig. 1a and b). A recent work⁷ has added one point on this line at large negative pressure, but this was not enough to decide between the two scenarios. Another, singularity-free scenario, also predicts peaks instead of divergence, but without a liquid-liquid transition (LLT)⁸. Up to now, despite tremendous efforts⁹, experiments have failed to detect a LLT or peaks in bulk supercooled water: crystallization always occurred before any extremum is reached.

Measurements on a metastable liquid are difficult to perform. In bulk water at positive pressure, decisive experiments to discriminate between the proposed scenarios have been precluded by unavoidable crystallization. To circumvent this problem, water proxies have been used: water confined in narrow pores¹⁴, or bulk water-glycerol mixtures¹⁵. Although the results supported the second critical point interpretation, their relevance to bulk water is not straightforward.

Here we study bulk water samples, a few microns in diameter, in the doubly metastable region: the liquid is simultaneously supercooled and exposed to mechanical tension or negative pressure. Negative pressures occur in nature, e.g. in the sap off trees, under the tentacles of octopi, or in fluid inclusions in minerals^{16,17}. The study of the largest tensions achievable in water was pioneered by the group of Angell¹⁰. They used a ‘Berthelot tube’ technique (Fig. 1c), based on isochoric cooling of a micrometer size inclusion of water in quartz. Tensions as large as -140 MPa have been reported, and confirmed by others^{7,11,12}, which exceed by far the limit of other techniques^{16,17}. It was already recognized in the work of Angell that the high density water inclusions that were able to survive cooling to room temperature without cavitation were also able to be supercooled below 0°C . Indeed, when the isochore crosses the line of density maxima of water, the tension is released and cavitation becomes less likely. Another study¹⁸ using macroscopic Berthelot tubes also reached the doubly metastable region, but the tensions were around -10 MPa only.

In order to reach large tensions, we use two microscopic inclusions of water in quartz (Fig. 1d, inset)¹³. We perform Brillouin light scattering experiments on these samples; this technique gives access to the sound velocity within the liquid¹³. Several Brillouin light scattering studies on supercooled water at ambient pressure are available^{19–24}, but only one work investigated water under tension¹¹: all samples in that study cavitated above room temperature except one with a density close to that of our sample 1. However, measurements in Ref. 11 were reported only down to 0°C , and the direct comparison to an extrapolated EoS was not considered. Our work extends the covered range to supercooled water under tension, reporting measurements down to -15°C along two isochores at $\rho_1 = 933.2 \pm 0.4\text{ kg m}^{-3}$ and $\rho_2 = 952.5 \pm 1.5\text{ kg m}^{-3}$, and reaching pressures beyond -100 MPa (supplementary online text). Representative spectra are shown in Fig. 1d. Such spectra are analyzed to give the zero frequency sound velocity c ¹³. To support the experimental results, we also perform molecular dynamics simulations of c with TIP4P/2005 water²⁵ at the same thermodynamic conditions¹³.

Figure 2 shows the experimentally measured and the numerically computed values of c as a function of tempera-

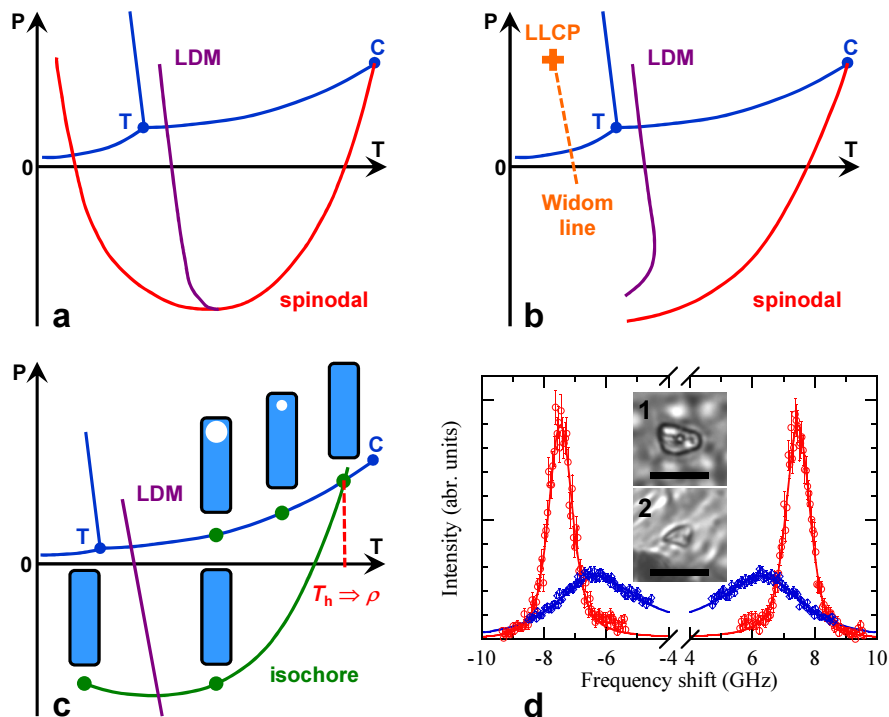


FIG. 1: **Scenarios and experiments for metastable liquid water.** **a**, Stability-limit conjecture². A schematic phase diagram for water is shown in the pressure-temperature plane with equilibrium transitions between liquid, vapor and ice (blue curves); T is the triple point and C the liquid-vapor critical point. If the LDM reaches the liquid-vapor spinodal at negative pressure, the latter bends to lower tension at lower temperature. This would provide a line of instability at positive pressure responsible for the anomalies observed in supercooled water. **b**, In the second critical point interpretation⁴, the LDM bends to lower temperatures at larger tension, and the spinodal remains monotonic. The anomalies of supercooled water are due to the vicinity of a liquid-liquid critical point (LLCP). Thermodynamic functions exhibit a peak near the Widom line emanating from the LLCP^{5,6}. **c**, Berthelot tube method^{7,10–12}. A closed, rigid container with a fixed amount of water is heated until the last vapor bubble disappears at T_h . Upon cooling, the bubble does not reappear and the liquid follows an isochore (green curve) and is put under mechanical tension. If the density is high enough, cavitation does not occur and the liquid can reach the doubly metastable region, where water is both supercooled and under tension. **d**, Typical Brillouin spectra. They were obtained with the homogenized sample 1 at 140°C (red circles) and -12°C (blue diamonds). The solid curves are fits used to obtain the sound velocity¹³. Note that the -12°C spectrum was rescaled to the same exposure time as the 140°C spectrum for easier comparison. The samples are shown as inset (scale bars, 10 μm).

ture at several thermodynamic conditions. Let us first describe the measurements on sample 1 after cavitation, at temperatures up to $T_{h,1}$: at these conditions the liquid is in equilibrium with its vapor. The measured sound velocity is in excellent agreement with the known sound velocity along the binodal and with our simulations of TIP4P/2005 water along its binodal²⁶. The agreement between simulations and tabulated experimental data also illustrates the quality of the potential used to simulate water²⁵. When the temperature of sample 1 reaches $T_{h,1}$, the last vapor bubble disappears leaving the inclusion entirely filled with liquid at density ρ_1 . Upon further heating, the pressure increases along the ρ_1 isochore. Once more, the measurements agree with the sound velocity from the known EoS and from our simulations along the ρ_1 isochore. Note that the measurements leave the binodal exactly at $T_{h,1}$, which has been determined independently by direct observation under the microscope. These consistency further corroborates the robustness of our data.

Next, we make sample 1 metastable by cooling along the ρ_1 isochore. We observe that below $T_{h,1}$, the measured sound velocity starts diverging with respect to the one extrapolated using the IAPWS EoS. In contrast, it agrees with our simulations. The IAPWS EoS predicts a re-entrant liquid-vapor spinodal: in this case, one would expect the sound velocity curve to reach a small value when the isochore approaches the spinodal at low temperature (for ρ_1 , the IAPWS EoS predicts that they meet at -33.5°C with $c = 829 \text{ m s}^{-1}$). In contrast, both experiments and simulations give a sound velocity that reaches a minimum near 0°C , before increasing on further cooling. Therefore, the isochore at ρ_1 does not approach the liquid-vapor spinodal as expected from the IAPWS EoS. Since we follow an isochore, the sound velocity minimum corresponds to a maximum in the adiabatic compressibility. Eventually, the sound velocity reaches a value *higher* than the value that one would expect along the binodal at -15°C , even though ρ_1 lies *below*

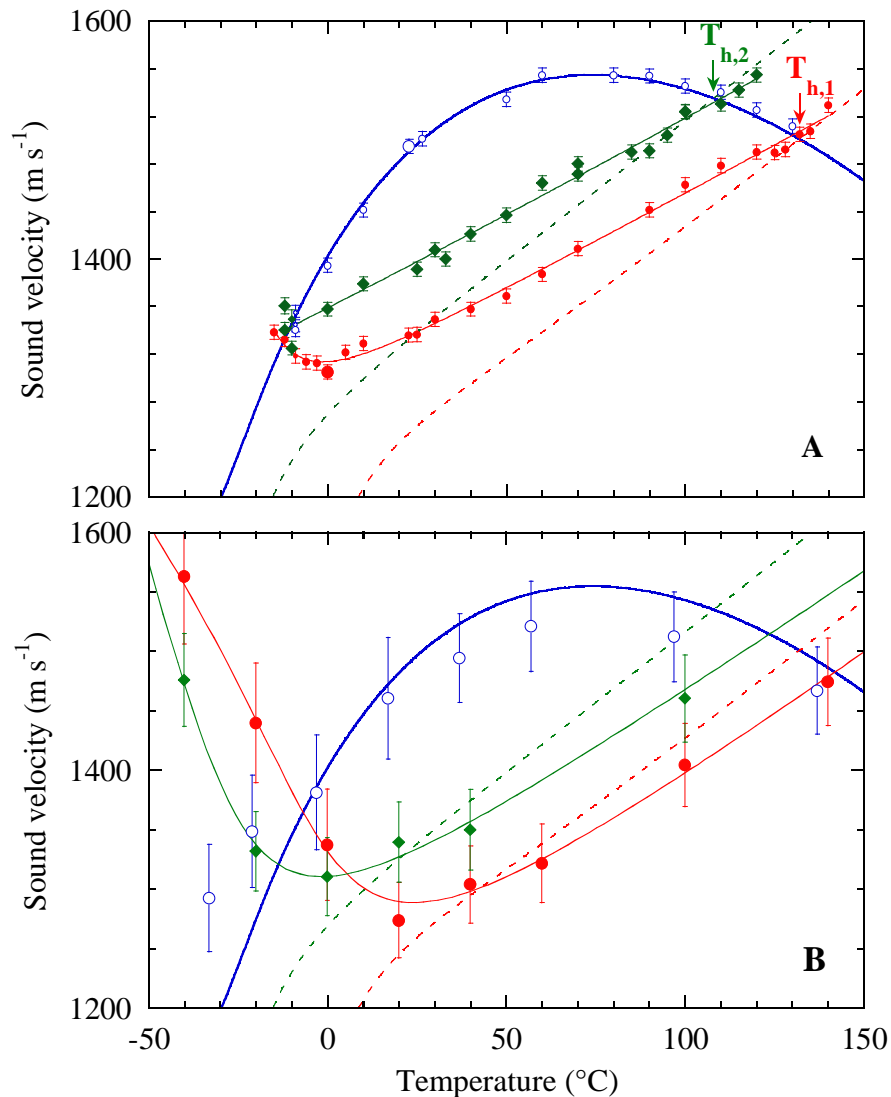


FIG. 2: **Sound velocity as a function of temperature.** The IAPWS EoS is used to plot the sound velocity along the binodal (thick blue curve) and along the isochores at ρ_1 (dashed red curve) and ρ_2 (dashed green curve). **A**, comparison with experiments. The symbols show our measurements on sample 1 after cavitation (open blue circles) and on metastable samples 1 (filled red circles) and 2 (filled green diamonds). The three symbol sizes correspond to three pinhole sizes on the spectrometer. The solid red and green curves are guides to the eye. The arrows show the homogenization temperatures of samples 1 and 2 as observed under the microscope. **B**, comparison with simulations of TIP4P/2005 water. The sound velocity was calculated along the TIP4P/2005 binodal (open blue circles), and the isochores at ρ_1 (filled red circles) and ρ_2 (filled green diamonds). The solid red and green curves are guides to the eye. Whereas the IAPWS EoS predicts a monotonic variation of c along the isochores, both experiments and simulations find that c reaches a minimum and increases above the values on the binodal at low temperature.

the liquid density on the binodal, $\rho_0 = 996.3 \text{ kg m}^{-3}$ at -15°C (ref. 27).

To confirm our results, we have repeated measurements and simulations on sample 2 with a higher density ρ_2 . We find a similar deviation from the extrapolation of the IAPWS EoS. In the simulations, the sound velocity reaches a minimum, which is not clear in the experiments that seem to reach a plateau. This is consistent with the fact that the simulations find the minimum for ρ_2 at a temperature lower than for ρ_1 , while for ρ_1 the experiment finds the minimum at a temperature lower than the simulations. Therefore it is likely that the minimum for ρ_2 lies at temperatures below the one reached in the experiment. In both experiment and simulations, while at -12°C ρ_2 is *between* ρ_1 and ρ_0 , the corresponding sound velocity is even slightly *higher* than both. Therefore, the sound velocity must reach a minimum between ρ_2 and ρ_0 along the -12°C isotherm. This is more clearly seen on Fig. 3: the sound velocity at ρ_0 , ρ_1 and ρ_2 virtually fall on a horizontal line, but the slope of $c(\rho)$ at ρ_0 necessarily implies a minimum.

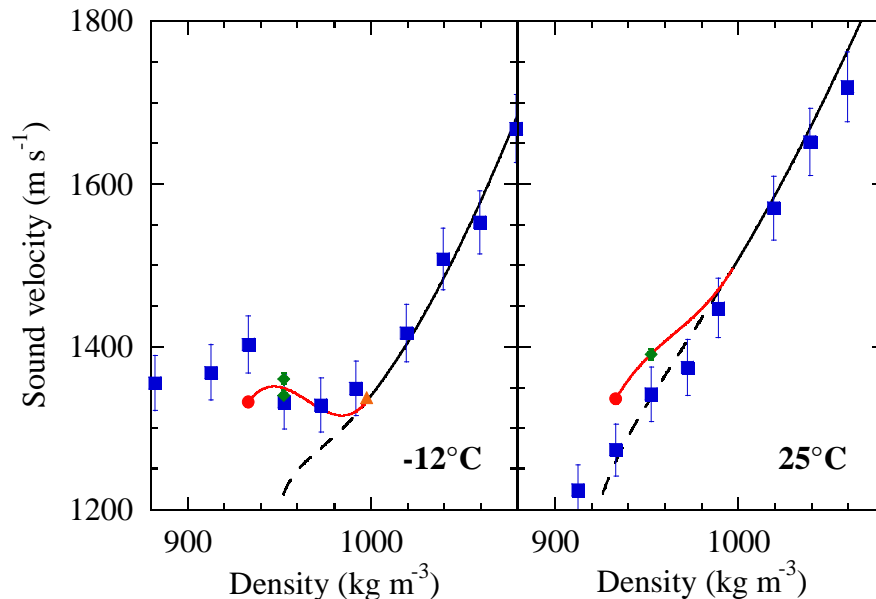


FIG. 3: **Sound velocity versus density at -12°C and 25°C .** The IAPWS EoS is shown in black, as a solid curve above the binodal, and as a dashed curve for its extrapolation to lower density. Our measurements for ρ_1 and ρ_2 are shown as filled red circles and green diamonds, respectively. The red curves are guides to the eye chosen to connect the data to the IAPWS EoS above the binodal with the correct slope. Note that the IAPWS EoS reproduces accurately experimental data above the binodal for stable water (e.g. at 25°C), and data along the binodal for supercooled water (e.g. at -12°C). To illustrate the latter, we have included in the left panel the experimental value of the sound velocity at -11.2°C (orange triangle) from ref. 23 (see SOM text). The solid blue squares give the results of the simulations of TIP4P/2005 water; note that the simulations in the right panel were obtained at 20°C . At high temperature, measurements and simulations agree with the IAPWS EoS, whereas at low temperature, they suggest the occurrence of a minimum and maximum which are absent from the extrapolation of the IAPWS EoS.

This observation agrees with the predictions of the simulations but contrasts those of the IAPWS EoS.

To explain the observed anomalies, it is interesting to look for other systems with a minimum in $c(\rho)$ along an isotherm. This actually occurs in all fluids, in their supercritical phase: the sound velocity at a temperature above the liquid-vapor critical temperature passes through a minimum when the density crosses the critical density (see for instance Fig. 8 of Ref. 28 for methanol and ethanol). Based on this observation, we propose that the anomalies of the sound velocity, observed both in experiments and in simulations, are a signature of supercritical phenomena. Here, in addition, the sound velocity reaches a maximum when the density decreases (Fig. 3). This is because eventually the liquid-vapor spinodal density has to be reached, and the sound velocity has then to become small. The simulations can then be used as a guide to better understand the origin of such anomalies. Several potentials predict a LLT in the supercooled region, ending at a LLCP. Based on the locus of maxima of κ_T along isobars, a LLCP for TIP4P/2005 has been proposed at $T_c = 193\text{ K}$, $P_c = 135\text{ MPa}$, and $\rho_c = 1012\text{ kg m}^{-3}$ ²⁹. Water above 193 K would thus be in a supercritical state associated to the LLT.

One may wonder why all previous experiments at positive pressure failed to detect a peak in thermodynamic functions. Simulations with a LLT show that specific quantities (such as isothermal compressibility κ_T or isobaric heat capacity) reach a peak on different lines, but that these lines all come close to each other and to the Widom line near the LLCP⁶. The locus of maxima for κ_T along isobars ($\text{LM}\kappa_T$) has been recently computed for TIP4P/2005 water at positive pressure²⁹. We have now computed this line also at negative pressure (supplementary online text). The results are shown on Fig. 4 and compared to the isochores we studied and to the experimental line of homogeneous crystallization³⁰. At positive pressure, the $\text{LM}\kappa_T$ is not accessible to experiments since it lies in the so-called ‘no man’s land’³¹, a region where bulk liquid water cannot be observed experimentally. However, at negative pressure, the slope of the $\text{LM}\kappa_T$ becomes less negative than that of the line of homogeneous crystallization. Since the latter keeps the same slope, the $\text{LM}\kappa_T$ line leaves the ‘no man’s land’ and enters the doubly metastable region that we have now shown is accessible to quantitative experimentation.

Is there a way to directly observe the LLT? If it exists, it is likely to lie in the ‘no man’s land’. Therefore it will be hard to decide between the second critical point interpretation and the singularity free scenario⁸; note however that the latter can be seen³² as a LLT with a critical point at 0 K. What our results do show is that the liquid-vapor

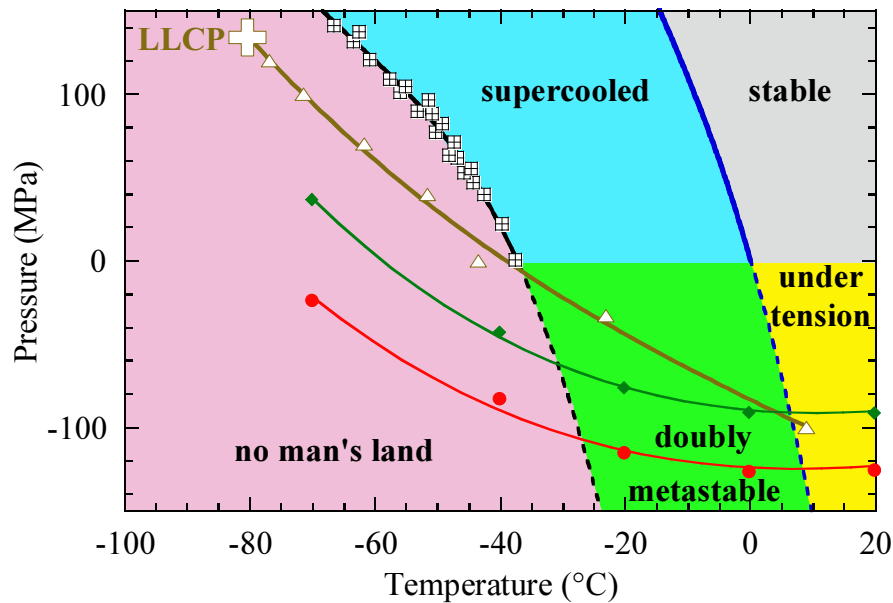


FIG. 4: **Pressure-temperature phase diagram of water.** Colored areas are used to identify the different possible states for liquid water. The melting line of ice Ih is shown at positive pressure by a solid blue curve and its extrapolation to negative pressure by a dashed blue curve. The black crossed squares show the experimental supercooling limit³⁰. They define the experimental homogeneous nucleation line (solid black curve), which is extrapolated here to negative pressure (dashed black curve). The ρ_1 and ρ_2 isochores of TIP4P/2005 water are shown by the red circles and curve, and green diamonds and curve, respectively. Simulations of TIP4P/2005 water are performed to find the maximum κ_T along several isobars (white triangles), defining the $LM\kappa_T$ (brown curve), that might emanate from a liquid-liquid critical point (LLCP, white plus symbol). The $LM\kappa_T$ becomes accessible to experiments in the doubly metastable region only.

spinodal does not reach the location predicted by extrapolation from the IAPWS EoS, and that the measured sound velocity quantitatively agrees with the one obtained with simulations of TIP4P/2005 water, which predicts a LLT. The doubly metastable region therefore appears like a promising experimental territory to test other predictions from the models proposed to explain water anomalies.

-
- ¹ R. J. Speedy, C. A. Angell, *J. Chem. Phys.* **65**, 851 (1976).
 - ² R. J. Speedy, *J. Phys. Chem.* **86**, 982 (1982).
 - ³ The International Association for the Properties of Water and Steam, Revised release on the IAPWS formulation 1995 for the thermodynamic properties of ordinary water substance for general and scientific use (2009).
 - ⁴ P. H. Poole, F. Sciortino, U. Essmann, H. E. Stanley, *Nature* **360**, 324 (1992).
 - ⁵ F. Sciortino, P. H. Poole, U. Essmann, H. E. Stanley, *Phys. Rev. E* **55**, 727 (1997).
 - ⁶ L. Xu, *et al.*, *Proceedings of the National Academy of Sciences of the United States of America* **102**, 16558–16562 (2005).
 - ⁷ M. El Mekki Azouzi, C. Ramboz, J.-F. Lenain, F. Caupin, *Nat Phys* **9**, 38 (2013).
 - ⁸ S. Sastry, P. G. Debenedetti, F. Sciortino, H. E. Stanley, *Physical Review E* **53**, 6144–6154 (1996).
 - ⁹ P. G. Debenedetti, H. E. Stanley, *Phys. Today* **56**, 40 (2003).
 - ¹⁰ Q. Zheng, D. J. Durben, G. H. Wolf, C. A. Angell, *Science* **254**, 829 (1991).
 - ¹¹ A. D. Alvarenga, M. Grimsditch, R. J. Bodnar, *J. Chem. Phys.* **98**, 8392 (1993).
 - ¹² K. I. Shmulovich, L. Mercury, R. Thiéry, C. Ramboz, M. El Mekki, *Geochimica et Cosmochimica Acta* **73**, 2457 (2009).
 - ¹³ Materials and methods are available as supporting material.
 - ¹⁴ D. Liu, *et al.*, *Proceedings of the National Academy of Sciences* **104**, 9570 (2007).
 - ¹⁵ K.-I. Murata, H. Tanaka, *Nature Materials* **11**, 436 (2012).
 - ¹⁶ F. Caupin, E. Herbert, *Comptes Rendus Physique* **7**, 1000 (2006).
 - ¹⁷ F. Caupin, A. D. Stroock, *Liquid polymorphism*, H. E. Stanley, S. Rice, eds., no. 152 in *Advances in Chemical Physics* (Wiley, New York, 2013).
 - ¹⁸ S. Henderson, R. Speedy, *Journal of Physics E: Scientific Instruments* **13**, 778 (1980).
 - ¹⁹ J. Teixeira, J. Leblond, *J. Physique Lett.* **39**, 83 (1978).
 - ²⁰ O. Conde, J. Leblond, J. Teixeira, *Journal de Physique* **41**, 997 (1980).

- ²¹ O. Conde, J. Teixeira, P. Papon, *The Journal of Chemical Physics* **76**, 3747 (1982).
²² G. Maisano, *et al.*, *Physical Review Letters* **52**, 1025–1028 (1984).
²³ S. Magazu, *et al.*, *The Journal of Physical Chemistry* **93**, 942 (1989).
²⁴ A. Cunsolo, M. Nardone, *The Journal of Chemical Physics* **105**, 3911 (1996).
²⁵ J. L. F. Abascal, C. Vega, *The Journal of Chemical Physics* **123**, 234505 (2005).
²⁶ C. Vega, J. L. F. Abascal, I. Nezbeda, *The Journal of Chemical Physics* **125**, 034503 (2006).
²⁷ D. E. Hare, C. M. Sorensen, *The Journal of Chemical Physics* **87**, 4840 (1987).
²⁸ T. Ohmori, Y. Kimura, N. Hirota, M. Terazima, *Physical Chemistry Chemical Physics* **3**, 3994 (2001).
²⁹ J. L. F. Abascal, C. Vega, *The Journal of Chemical Physics* **133**, 234502 (2010).
³⁰ H. Kanno, R. J. Speedy, C. A. Angell, *Science* **189**, 880 (1975).
³¹ O. Mishima, H. E. Stanley, *Nature* **396**, 329–335 (1998).
³² K. Stokely, M. G. Mazza, H. E. Stanley, G. Franzese, *Proceedings of the National Academy of Sciences* **107**, 1301 (2010).

Acknowledgments

Acknowledgements We thank C. Austen Angell and José Teixeira for discussions; Véronique Gardien for providing us with sample 2; and Abraham D. Stroock and Carlos Vega for suggestions to improve the manuscript. The team at Lyon acknowledges funding by the ERC under the European Community’s FP7 Grant Agreement 240113, and by the Agence Nationale de la Recherche ANR Grant 09-BLAN-0404-01. C.V. acknowledges financial support from a Marie Curie Integration Grant PCIG-GA-2011-303941 ANISOKINEQ and thanks the Ministerio de Educacion y Ciencia and the Universidad Complutense de Madrid for a Juan de la Cierva fellowship. The team at Madrid acknowledges funding from the MCINN Grant FIS2010-16159.

Supplementary Materials Materials and Methods. SOM Text. Figs. S1 to S7. Table S1 to S3.